ISSN 1063-7834, Physics of the Solid State, 2022, Vol. 64, No. 8, pp. 467–473. © Pleiades Publishing, Ltd., 2022.
ISSN 1063-7834, Physics of the Solid State, 2022. © Pleiades Publishing, Ltd., 2022.
Russian Text © The Author(s), 2022, published in Fizika Tverdogo Tela, 2022, Vol. 64, No. 9, pp. 1188–1195.

Experimental Study of Elements of a Josephson Traveling-Wave Parametric Amplifier on SQUID Chains

R. A. Yusupov[a, *], L. V. Filippenko[a], M. Yu. Fominskiy[a], and V. P. Koshelets[a]

[a] *Kotel'nikov Institute of Radio Engineering and Electronics, Russian Academy of Sciences, Moscow, 125009 Russia*

**e-mail: yusupovrenat@hitech.cplire.ru*

Received April 29, 2022; revised April 29, 2022; accepted May 12, 2022

Abstract—The issues of designing a Josephson traveling-wave parametric amplifier (JTWPA) based on a well-established technology of superconducting microcircuits with given and controlled parameters based on high-quality Nb–AlO_x–Nb tunnel junctions are considered. This technology has been adapted and optimized to obtain structures with the required parameters and circuits with large number of tunnel junctions. To advance the technology, the basic elements of a promising JTWPA have been developed, manufactured and studied. In direct current measurements, a number of superconducting elements parameters were experimentally determined; these parameters are required for designing a JTWPA chips for microwave measurements. An original design of JTWPA based on a chain of SQUIDs in a coplanar line has been developed for implementation using niobium technology of the Kotel'nikov Institute of Radio Engineering and Electronics, Russian Academy of Sciences. The parameters of the main elements of the JTWPA have been determined.

Keywords: Josephson travelling-wave parametric amplifiers (JTWPA), Josephson metamaterials (JMM), Josephson junctions (JJs), cold amplifier, coplanar lines, quantum noise, SIS junctions, SQUID

DOI: 10.1134/S1063783422090086

1. INTRODUCTION

Currently, there is growing interest in the development of various quantum devices (qubits, detectors with a quantum level of sensitivity, etc.), which operate at low and ultralow temperatures at frequencies of a few and a few tens of gigahertzes according to their nature. To communicate with quantum systems, components and devices that can operate at ultralow temperatures and allow one to control, process, and read information, as well as to amplify weak high frequency signals, are needed. The practical parameters of linear semiconductor microwave amplifiers have reached the limit values and do not allow one to obtain the bandwidth, gain, and noise required to develop systems for reading qubits in a quantum computer, axion detectors, intermediate frequency amplifiers for radio astronomy heterodyne receivers, and readout systems for cryogenic bolometer arrays with frequency division of channels. The use of Josephson tunnel junctions (JJs) makes it possible to realize a lossless nonlinear inductance and provides characteristics that are unattainable for dissipative nonlinear components. It is possible to reduce the noise temperature below the quantum limit in the mode of compression of quantum states in case of implementing the phase-sensitive Josephson amplifier under consideration. It is assumed that the development of a fundamentally new type of broadband microwave traveling wave amplifier will make it possible to bypass the bandwidth and dynamic range limitations that exist for a traditional lumped component parametric amplifier and to reduce noise below the quantum limit [1].

Josephson parametric amplifiers [2] are considered the most advanced devices for fine experiments in the field of quantum measurements and quantum information technologies, but so far they have not received wide attention. Interest in these devices increased after the demonstration of a parametric traveling wave amplifier based on the kinetic inductance of a thin superconducting film [3]. However, the greatest attention of research groups in recent years has been attracted by Josephson parametric amplifiers in the traveling wave mode, which provide a higher gain per unit length at a lower pumping power on the basis of arrays of high-frequency (RF) or direct current (DC) SQUIDs [4–7]. In contrast to lumped Josephson parametric amplifiers with a limited amplifying band, JTWPAs provide the interaction between a signal and pumping along the entire length of the microband line and extend the bandwidth and the dynamic range of the amplifier.

In [8], Zorin predicted the possibility of creating a Josephson travelling-wave parametric amplifiers (with a number of components in the range of 300–600), which can provide a gain in the region of 20 dB in the band of 4–8 GHz (see Fig. 1a). Later studies [9] were

no longer so optimistic and discussed about achieving a gain of 7–10 dB in a wide band with a reasonable number of cells of 1175. The first implementation in broadcasting [10] showed the fundamental possibility of creating this type of amplifier, and its modernization performed in HYPRES demonstrated an average gain of about 10 dB in this band, but with fairly strong frequency response unevenness [11]. A working prototype of such an amplifier based on niobium SIS junctions was implemented using a technology with a current density of 100 A/cm^2; symmetrical RF SQUIDs with Josephson junctions with a nominal critical current of 4 to 12 μA were studied.

To date, the noise temperature have not been measured, which should be less than 1 K at an operating temperature of 4.2 K, according to theory. A prototype of such an amplifier operating at millikelvin temperatures and having a noise temperature close to the quantum limit, i.e., less than 0.5 K at 8 GHz, has not been developed.

2. DESIGN AND ENGINEERING OF JTWPAs

We have developed a symmetrical design of the JTWPA line (Fig. 1b) and separate test structures for determining the inductive parameters of the components. The critical junction current in real samples is determined by a combination of the following two factors: the first factor is R_nS, i.e., a parameter determined by the conditions for the formation of a tunneling barrier; the second factor is S, i.e., the area of the junction itself (it is more convenient to talk about the linear size characterized by diameter d_j). A unified size of the JJ with a diameter of $d_j = 2$ μm (round junctions) is chosen; the parameter of the three-layer structure is $R_n = 1000\ \Omega/\mu m^2$. The corresponding critical current is estimated to be $I_c = 5.3$ μA, given that Nb is a strongly coupled superconductor and the actually measured critical current (I_c) of the junctions is a 0.5–0.6 fraction of the current surge at gap voltage (I_g). The normal resistance of such a junction (R_n) is estimated to be 320 Ω and the junction capacitance is $C_j = 160$ fF. Reducing the size of the junction would make it possible to achieve a smaller critical current, but it is critical to create arrays of junctions with a small relative spread of critical currents for the operation of the JTWPA.

To evaluate the optimal parameters of the JTWPA design based on RF SQUIDs, a calculation algorithm was developed in the MathCAD software environment. The main parameter of the JTWPA is SQUID's dimensionless inductance $\beta_L \equiv 2\pi L_g I_c/\Phi_0$ [8], where L_g is the geometric inductance, must be less than 1 for the hysteresis-free shape of the current–voltage characteristic, and tends to 1 for the optimal amplification of each individual cell. The value of geometric inductance L_g is determined by the size and geometry of the SQUID loop, but determining the exact values analytically in such circuits is a rather difficult problem. In our scheme, square-shaped SQUIDs are chosen; they are easier to design and calculate, and they provide a fairly dense arrangement of cells. The loop width of the SQUID is 4 μm; this linewidth is reliably and accurately obtained within the framework of the technology used.

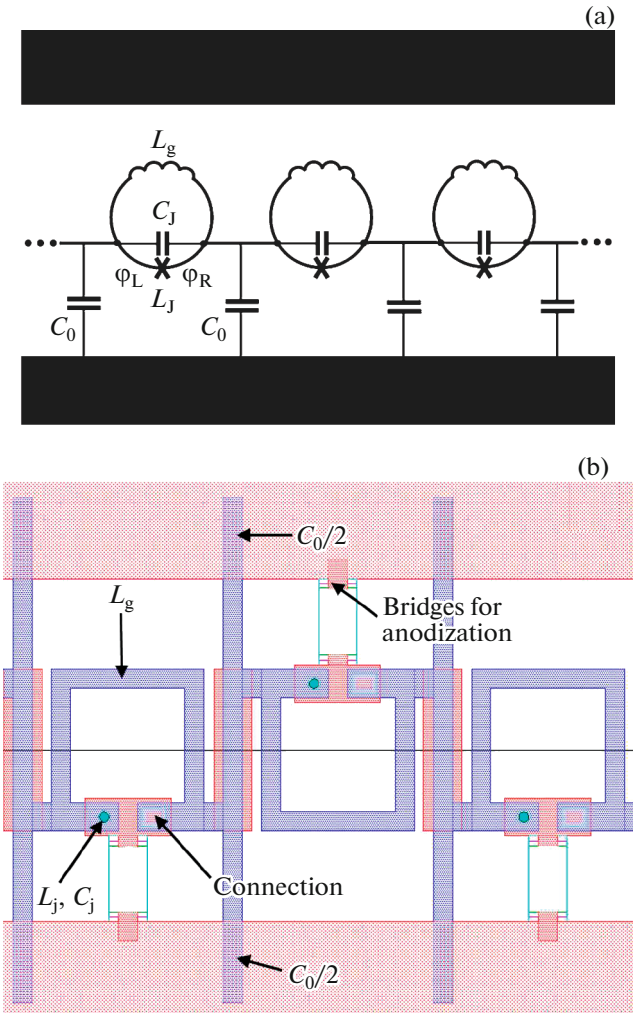

Fig. 1. (a) Circuit scheme of the transmission line, including an array of RF SQUIDs; the Josephson junction is represented as a parallel connection of the Josephson inductance (L_j) and the tunnel capacitor (C_j). (b) View of the developed line geometry with RF SQUIDs.

For a more accurate numerical calculation of inductances, the InductEx software was used, which was developed for calculating superconducting circuits. The inductances (L_g) calculated in this fashion turned out to be higher (57 pH) than those calculated using a simple analytical formula of $1.25\mu_0 d$ for a square frame (37.5 pH), in which there is a dependence only on the internal size of the loop. To achieve the desired geometric inductance, the calculated side of the square frame was 24 μm. Capacitance C_0 to

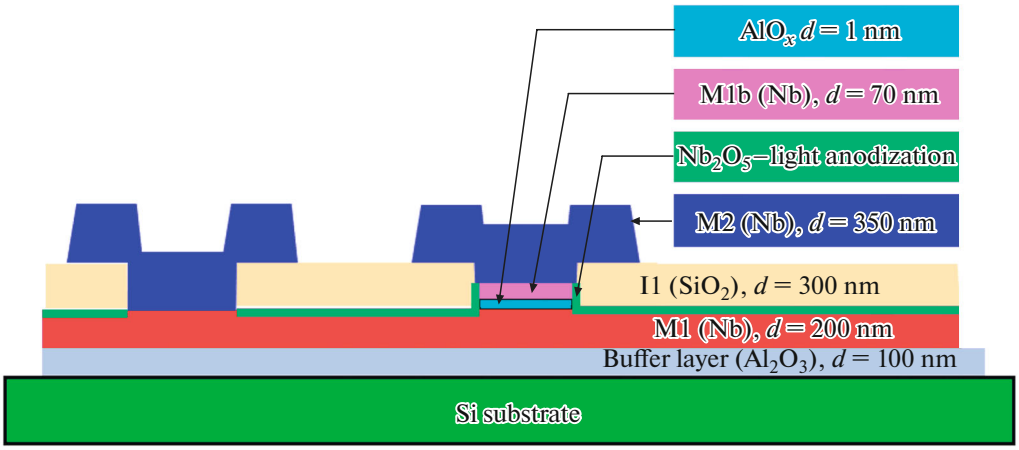

Fig. 2. Cross section of an integrated circuit with two superconducting layers.

ground must provide an impedance of $Z_0 = (L/C)^{1/2}$ for each cell close to 50 Ω in order to match with transmission lines, and cutoff frequency $f_0 = (LC)^{-1/2}$ must be sufficiently low. The calculated capacitance per cell should be 23 fF; in the developed design, it is achieved by two symmetrical overlapping regions of the superconducting layers with earth conductors of the coplanar line.

For a three-frequency operation with signal frequency $f_s \sim 0.5f_p$, the gain of a cell structure comprised of N cells is estimated to be $G = \cosh^2(g_0N)$, where the exponential gain factor is $g_0 = |\chi|(\beta_L I_p/4I_c)(f_p/f_0)$. For the calculated amplifier line with $\beta_L = 0.9$, the number of cells to achieve a desired gain of 20 dB was at least 700 pieces. Similarly, parameters for two-contact DC SQUIDs, with other loop sizes, and for variants with shunted Josephson junctions are calculated.

For the designed arrays of SQUIDs, the optimal parameters of the coplanar line in which they are located are calculated. For samples on silicon high-resistance substrates (ρ > 10 kΩ cm) with a thickness of 0.5 mm with a metal (Nb) screen on the reverse side with a thickness of 0.2 μm and a central line width of 34 μm, the optimal gap to grounded conductors was 19 μm.

3. TECHNIQUES FOR PRODUCING SAMPLES WITH TEST STRUCTURES

At the Kotel'nikov Institute of Radio Engineering and Electronics, a technological facility for the manufacture of superconducting structures based on high-quality Nb–AlO$_x$–Nb tunnel junctions successfully operates, which makes it possible to fabricate structures in micron and submicron sizes with a tunnel current density of 0.1–10 kA/cm^2 [12–14]. This technology has been adapted to fabricate samples with two superconducting layers, anodization, and an additional insulation layer to reliably prevent short circuits (see Fig. 2). The key requirements for the technology are a relatively low tunnel current density (approximately 0.3 kA/cm^2), the possibility of creating structures with a large number of JJs (up to 1000), and small relative spreads in the parameters of these junctions. Additionally, the possibility of deposition of shunt resistances for test measurements was provided. The capacitance to ground, which is necessary for the implementation of the amplifier line, is proposed to accomplish using insulator layer I1; this capacitance has an estimated value of 0.17 fF/μm^2.

All film deposition procedures were carried out by magnetron sputtering. First, a thin (100 nm) Al$_2$O$_3$ buffer layer was deposited; this sublayer is a stop layer for etching a three-layer structure. After that, a three-

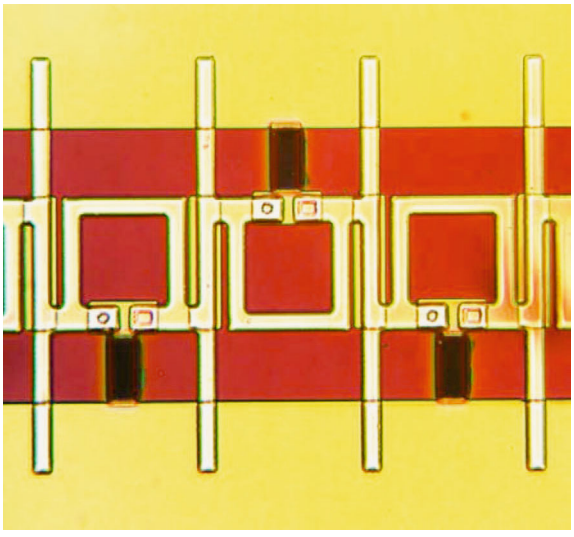

Fig. 3. View of the fabricated array of RF SQUIDs in a coplanar line.

Table 1. Parameters for deposition of film layers

Layer	Template	Material	Layer description	Thickness, nm
		Al_2O_3	Buffer layer	100
M1	Negative	$Nb/AlO_x/Nb$	Three-layer structure Nb base electrode–tunnel barrier AlO_x–Nb	200
			upper electrode	7
				200
I1	Negative	AlO_x/Nb	Formation of tunnel junction region by reactive ion etching (RIE)	80
		Nb_2O_5	Light anodization; 10 V	20
		SiO_2	SiO_2, dielectric; estimated capacitance 0.17 fF/μm^2 ± 25%	300
ETCH	Positive		Etching (Nb and AlO_x) for direct contact M1 with M2 (RIE + KOH)	
M2	Positive	Nb	Nb, superconductor; London penetration depth λ_L = 85 nm ± 5%	350
CONT	Positive	Al/Au	Contact pads	200
ALO	Positive		Final removal of anodizing bridges (RIE)	

layer $Nb/AlO_x/Nb$ structure was deposited in a single cycle without interrupting the vacuum; the corresponding layer thicknesses were 200, 7, and 80 nm. The geometry of the lower layer of the superconductor was formed by the method of lift-off photolithography using mask M1. The next operation was the formation of the region of tunnel junctions by etching from a three-layer structure using mask I1. The same resist mask is used for anodizing, first of all, the junction walls and for sputtering in the regions not covered by the 250 nm thick SiO_2 insulator resist, which provides a coating for the lower electrode to prevent electrical contact between the two superconducting layers. To contact two superconducting layers in the desired spots (previously they were also covered with a resist on mask I1), windows are formed by etching on mask ETCH. The next optional stage is the formation of shunts from Mo, which is a nonsuperconducting material at a temperature of 4.2 K. Shunted junctions are not required in the structures of real amplifiers and are used only in test structures. The structure of the second superconducting layer (M2) with a thickness of 350 nm is formed by the lift-off method. The last technological layer is comprised of gold contact pads with a thick of 200 nm. This structure is also created by the lift-off lithography method. For better adhesion of gold to niobium, a thin (1–2 nm) aluminum sublayer is used. The last stage is the removal of additional bridges that connect all regions with tunnel junctions by etching to anodize them. All film deposition parameters are given in Table 1.

Using this technology, two series of samples were produced, including separate single DC SQUIDs and arrays of RF and DC SQUIDs. For preliminary testing the manufactured microcircuits containing the prototypes of JTWPA components and evaluating the junction parameters, three test chips were included in the template, which were manufactured on the same substrate with working microcircuits. On each test microcircuit, several tunnel SIS junctions of different sizes (diameter from 2 to 4 μm) were made.

4. SCHEME AND RESULTS OF MESUREMENTS

The results of measurements of single test SIS junctions, as well as arrays and single DC SQUIDs at a temperature of 4.2 K are given. For the initial testing, a probe insert in a transport Dewar vessel with liquid helium was used, which made it possible to conduct quick testing of the manufactured samples. A substrate with the structures under study was attached to the measuring head of the cryogenic probe (fourteen contact pads are provided), the board with the sample was inside screens made of cryogenic permalloy and superconducting screen. Contacts were made using needles made of beryllium bronze that has a sufficient degree of elasticity at $T = 4.2$ K (see Fig. 4). The cur-

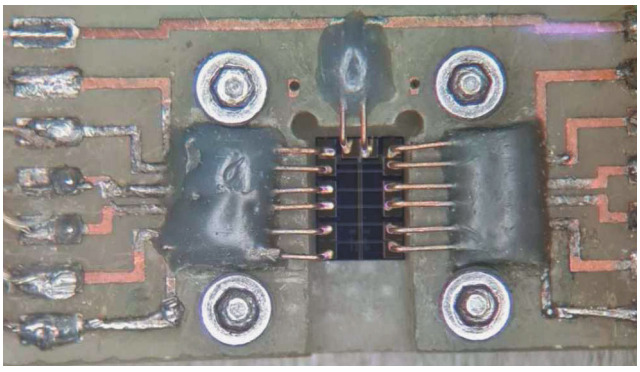

Fig. 4. View of the sample holder for preliminary testing of samples at a temperature of 4.2 K.

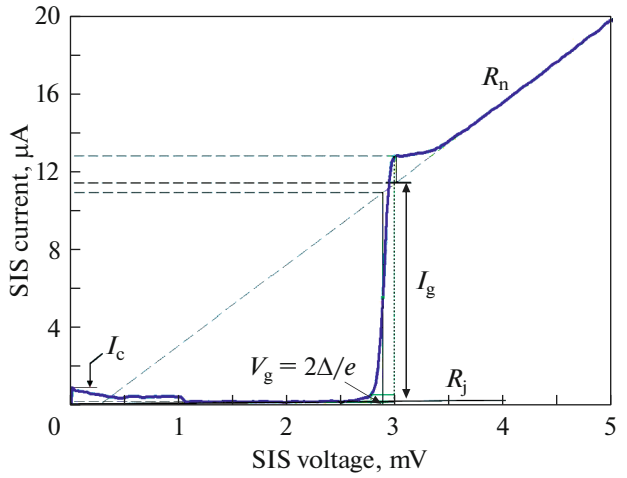

Fig. 5. Measured current–voltage characteristic for a single DC SQUID in the mode of setting the voltage with a suppressed critical current.

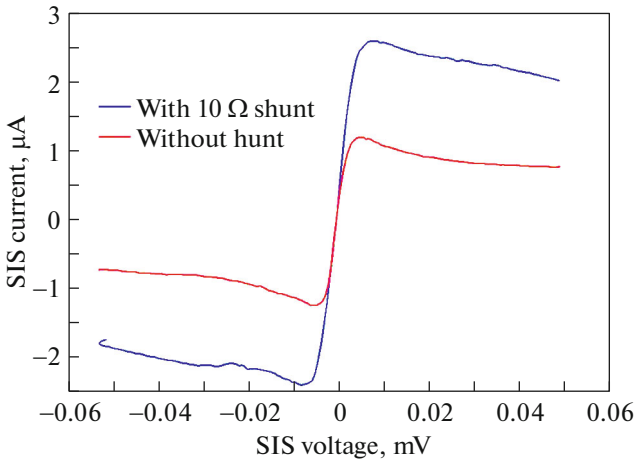

Fig. 6. Current–voltage characteristics recorded in the mode of setting the voltage with a critical current for a single DC SQUID.

rent–voltage characteristics (CVCs) were measured using a four-contact measuring method. The measurements were performed both in the mode of setting the voltage, which is used to better describe the features of the CVCs at voltages in the region of the gap, and in the mode of setting the current to more accurately record the critical current of the manufactured SIS structures. All junctions in all manufactured structures show high quality, the resistance ratio R_j/R_n is more than 45, and the same gap equal to V_g = 2.88 mV (see Fig. 5), which makes it possible to create high-quality Josephson metamaterials (JMM) using this technology.

In the JTWPA circuit based on SQUIDs, the key parameters are the geometric inductance of the SQUID loop and the critical junction current, on which the Josephson inductance depends. In the mode of setting the voltage with a current jump to a normal resistance, there is a so-called "knee-shaped" feature. It plays no role for the use of these tunnel structures in JMMs, since the values of the critical current are essential. Direct measurements of the critical current in such structures are strongly affected by external magnetic fields and electrical noises, so the measured values strongly depend on the parameters of the measurement system. For the described measurement system, the critical current values were higher in junctions shunted with a small (10 Ω) parallel resistance (see Fig. 6). The values of measured critical current I_c turn out to be noticeably smaller than the values of current surge I_g at target gap voltage V_g. The theoretical value of I_c/I_g for junctions with strongly coupling superconductors, such as niobium, is 0.5–0.6. In the measured test junction, this ratio depended on the junction area and ranged from 0.2 for small junctions to 0.55 for large junctions (see Table 2). First of all, we attribute this to the thermal noise of the SIS junction, which is 0.4–0.5 μA at a temperature of 4.2 K, and the presence of additional interference up to 1 μA in value for our nonoptimized test system. For junctions with a larger area and high critical currents, these mechanisms played a less important role.

Figure 7 shows the results of measuring the test DC SQUID structures exhibiting the modulation of the critical current and making it possible to determine the inductances of the components under study. The magnetic field in such structures was set by a direct current through an additional line at a distance of 19 μm from the SQUID loop. The ratios of the maximum and minimum current values to the current–flux characteristics of the SQUID depend on the ratio of the geometric and Josephson inductance, and the value of

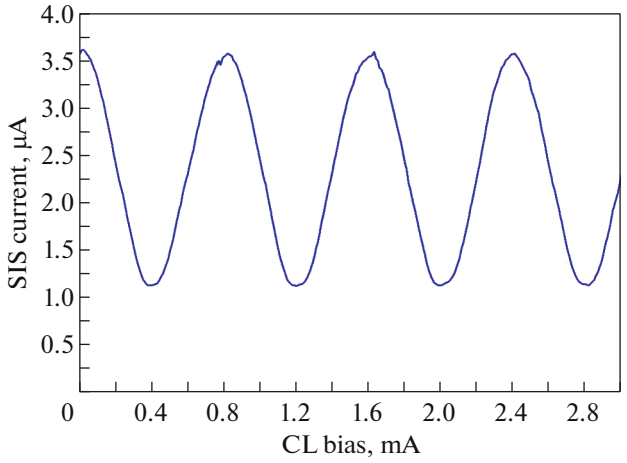

Fig. 7. Dependence of the current on the magnetic flux through the SQUID set by direct current passing through the control line.

Table 2. Measured values of critical currents for JJs of different sizes

d_j, μm	S, μm^2	R_j, Ω	I_g, μA	I_c, μA	I_c/I_g
8.73	59.83	35	74	40	0.54
4.73	17.56	120	21	9.2	0.44
4.23	14.05	150	17	6.8	0.40
3.73	10.92	194	13	4.7	0.36
3.23	8.19	257	10	2.5	0.25
2.73	5.85	349	7	1.5	0.21

dimensionless parameter β_L in this measurement was approximately 0.5, which is less than a value of 0.9 set in the design. These measurements also demonstrate the possibility of adjusting the SQUID line by passing the control current through the grounded conductors in the coplanar line.

For SQUID arrays, the measured CVCs also strongly depend on the configuration of the system, which complicates the estimation of the parameters of individual cells. The current–voltage characteristics of an array of twenty series-connected DC SQUIDs are shown as an example in Fig. 8, which were recorded with different magnetic field values leading to variation of critical current values in individual cells. The measured critical current for such a circuit were up to 3 μA per JJ and the I_c/I_g ratio ≈0.5 (excluding the knee-shaped feature just above the gap voltage). Therefore, one can focus on the current values at the gap voltage when designing a line based on RF SQUIDs.

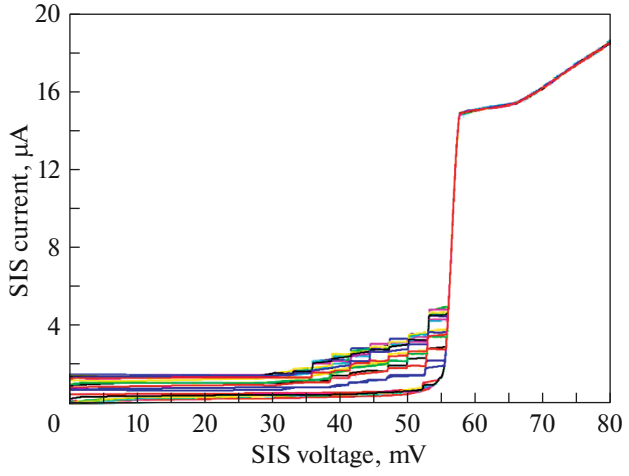

Fig. 8. Current–voltage characteristics recorded in the mode of setting the current at different current values (0–1 mA) in the control line for an array of twenty DC SQUIDs.

5. CONCLUSIONS

The main components for the implementation of the JTWPA based on SQUIDs have been developed and studied. An array of RF SQUIDs in a coplanar line is an option for the design of such a JTWPA. We have developed an original design of such an amplifier with use of the features of the Nb–AlO_x–Nb technology developed at the Kotel'nikov Institute of Radio Engineering and Electronics. For this, the optimal characteristics of the circuit are calculated taking into account the parameters depending on the selected technology regimes. The calculated value of the critical current of the Josephson junction is I_c = 5.3 μA. The optimal technological parameters (R_nS = 1000 Ω/μm^2) and junction areas (S = 3.14 μm^2) are determined, which allow one to obtain the required critical current.

The manufacturing technology is tested, the main parameters of the JTWPA components are measured, and their compliance with those included in the design are demonstrated. Schemes containing individual JTWPA components and units, such as single SQUIDs and their arrays included in coplanar lines, are developed. Manufactured structures with JJs demonstrate high quality characterized by R_j/R_n = 47 and a gap voltage of 2.88 mV, which make it possible to develop JTWPA structures on the basis of such junctions. Direct current measurements of the test structures show the difference between the measured parameters and the designed ones. This is due to the dependence of critical current I_c on the size of the junction in direct measurements in an insufficiently shielded system. Current jump values I_g at the gap voltage, which correspond to the designed values in the structures under study, are more indicative for arrays of RF SQUIDs in the JTWPA line.

Measurements of arrays of components with JJs have demonstrated the fundamental possibility of manufacturing such multicomponent structures with specified parameters and a small spread of parameter values. The possibility of pumping a signal into a SQUID line by passing the pump signal through grounded conductors in a coplanar line has been demonstrated; all these open up the possibility of implementing JTWPA on the basis of the existing niobium technology.

FUNDING

This study was supported by the Russian Science Foundation, project no. 21-42-04421. The tunnel junction structures were made using USU Cryointegral supported by a grant from the Ministry of Science and Higher Education of the Russian Federation (agreement no. 075-15-2021-667), within State assignment for the Kotel'nikov Institute of Radio Engineering and Electronics, Russian Academy of Sciences.

CONFLICT OF INTEREST

The authors declare that they have no conflicts of interest.

REFERENCES

1. Quantum Squeezing, Ed. by P. D. Drummond and Z. Ficek, Vol. 27 of *Springer Series on Atomic, Optical, and Plasma Physics* (Springer Science, New York, 2013).
2. B. Yurke, L. R. Corruccini, P. G. Kaminsky, L. W. Rupp, A. D. Smith, A. H. Silver, R. W. Simon, and E. A. Whittaker, Phys. Rev. A **39**, 2519 (1989).
3. B. Ho Eom, P. K. Day, H. G. LeDuc, and J. Zmuidzinas, Nat. Phys. **8**, 623 (2012).
4. K. O. Brien, C. Macklin, I. Siddiqi, and X. Zhang, Phys. Rev. Lett. **113**, 157001 (2014).
5. T. C. White, J. Y. Mutus, I. C. Hoi, R. Barends, B. Campbell, Y. Chen, Z. Chen, B. Chiaro, A. Dunsworth, E. Jeffrey, J. Kelly, A. Megrant, C. Neill, P. J. J. O'Malley, P. Roushan, D. Sank, A. Vainsencher, J. Wenner, S. Chaudhuri, J. Gao, and J. M. Martinis, Appl. Phys. Lett. **106**, 242601 (2015).
6. M. T. Bell and A. Samolov, Phys. Rev. Appl. **4**, 024014 (2015).
7. C. Macklin, K. O. Brien, D. Hover, M. E. Schwartz, V. Bolkhovsky, X. Zhang, W. D. Oliver, and I. Siddiqi, Science (Washington, DC, U. S.) **350**, 307 (2015).
8. A. B. Zorin, Phys. Rev. Appl. **6**, 034006 (2016).
9. T. Dixon, J. W. Dunstan, G. B. Long, J. M. Williams, P. J. Meeson, and C. D. Shelly, Phys. Rev. Appl. **14**, 034058 (2020).
10. A. B. Zorin, M. Khabipov, J. Dietel, and R. Dolata, in *Proceedings of the 16th International Superconductive Electron. Conference ISEC* (2017), p. 1.
11. A. Miano and O. A. Mukhanov, IEEE Trans. Appl. Supercond. **29**, 1501706 (2019).
12. O. Kiselev, M. Birk, A. Ermakov, L. Filippenko, H. Golstein, R. Hoogeveen, N. Kinev, B. vanKuik, A. de Lange, G. de Lange, P. Yagoubov, and V. Koshelets, IEEE Trans. Appl. Supercond. **21**, 612 (2011).
13. S. Butz, Supercond. Sci. Tech. **26**, 094003 (2013).
14. M. I. Faley, E. A. Kostyurina, K. V. Kalashnikov, Y. V. Maslennikov, V. P. Koshelets, and R. E. Dunin-Borkowski, Sensors **17**, 2798 (2017).

Translated by O. Kadkin